

RESEARCH PAPER

1E7-03, a low MW compound targeting host protein phosphatase-1, inhibits HIV-1 transcription

Tatyana Ammosova¹, Maxim Platonov^{2,3}, Andrei Ivanov¹, Yasemin Saygideğer Kont⁴, Namita Kumari¹, Kylene Kehn-Hall⁵, Marina Jerebtsova⁶, Amol A Kulkarni⁸, Aykut Üren⁴, Dmytro Kovalskyi^{2,4} and Sergei Nekhai^{1,7}

¹Center for Sickle Cell Disease, Department of Medicine, Howard University, Washington, DC, USA, ²ChemBio Center, National Taras Shevchenko University, Kiev, Ukraine, ³Enamine LLC, Princeton Corporate Plaza, Princeton, NJ, USA, ⁴Lombardi Comprehensive Cancer Center, Georgetown University, Washington, DC, USA, ⁵National Center for Biodefense and Infectious Diseases, School of Systems Biology, George Mason University, Manassas, VA, USA, ⁶Center for Genetic Medicine, Children's National Medical Center, Washington, DC, USA, ⁷Department of Microbiology, Howard University, Washington, DC, USA, and ⁸College of Pharmacy, Howard University, Washington, DC, USA

Correspondence

Sergei Nekhai, Center for Sickle Cell Disease, Howard University, 1840 7th Street, N.W. HURB1 Suite 202, Washington DC 20001, USA. E-mail: snekhai@howard.edu

Received

24 January 2014

Revised

7 June 2014

Accepted

14 June 2014

BACKGROUND AND PURPOSE

HIV-1 transcription is activated by the Tat protein which recruits the cyclin-dependent kinase CDK9/cyclin T1 to TAR RNA. Tat binds to protein phosphatase-1 (PP1) through the Q³⁵VCF³⁸ sequence and translocates PP1 to the nucleus. PP1 dephosphorylates CDK9 and activates HIV-1 transcription. We have synthesized a low MW compound 1H4, that targets PP1 and prevents HIV-1 Tat interaction with PP1 and inhibits HIV-1 gene transcription. Here, we report our further work with the 1H4-derived compounds and analysis of their mechanism of action.

EXPERIMENTAL APPROACH

Using the 1H4-PP1 complex as a model, we iteratively designed and synthesized follow-up libraries that were analysed for the inhibition of HIV-1 transcription and toxicity. We also confirmed the mechanism of action of the PP1-targeting molecules by determining the affinity of binding of these molecules to PP1, by analysing their effects on PP1 activity, disruption of PP1 binding to Tat and shuttling of PP1 to the nucleus.

KEY RESULTS

We identified a tetrahydroquinoline derivative, compound 7, which disrupted the interaction of Tat with PP1. We further optimized compound 7 and obtained compound 7c, renamed 1E7-03, which inhibited HIV-1 with low IC₅₀ (fivefold lower than the previously reported compound, 1H4), showed no cytotoxicity and displayed a plasma half-life greater than 8 h in mice. 1E7-03 bound to PP1 *in vitro* and prevented shuttling of PP1 into the nucleus.

CONCLUSIONS AND IMPLICATIONS

Our study shows that low MW compounds that functionally mimic the PP1-binding RVxF peptide can inhibit HIV-1 transcription by deregulating PP1.

Abbreviations

CTD, C-terminal domain of RNA polymerase II; HEXIM1, hexamethylene bis-acetamide-inducible protein 1; LTR, long terminal repeats; PP1, protein phosphatase 1; P-TEFb, positive transcription elongation factor b

Tables of Links

TARGETS
Enzymes
CDK (cyclin-dependent kinase)2
CDK9

LIGANDS
Microcystin-LR
Roscovitine (seliciclib)

These Tables list key protein targets and ligands in this article which are hyperlinked to corresponding entries in <http://www.guidetopharmacology.org>, the common portal for data from the IUPHAR/BPS Guide to PHARMACOLOGY (Pawson *et al.*, 2014) and are permanently archived in the Concise Guide to PHARMACOLOGY 2013/14 (Alexander *et al.*, 2013).

Introduction

Complete eradication of HIV-1 in infected individuals is hindered by the presence of a latent transcriptionally inactive HIV-1 provirus which cannot be targeted by existing anti-HIV-1 drugs (Lafeuillade and Stevenson, 2011). On the other hand, the emergence of drug-resistant HIV-1 in latently infected T-cells and macrophages presents a challenge as the therapeutic agents do not inhibit HIV-1 transcription. HIV-1 transcription from the HIV-1 long terminal repeats (LTR) depends both on host cell factors and on the HIV-1 transactivation Tat protein (see Nekhai *et al.*, 2013). HIV-1 Tat activates HIV-1 transcription by recruiting the positive transcription elongation factor b (P-TEFb) which contains the cyclin-dependent kinase CDK9/cyclin T1 to TAR RNA (Nekhai *et al.*, 2013). Inability of Tat to recruit CDK9/cyclin T1 to TAR RNA may contribute to the establishment of latency (Lafeuillade and Stevenson, 2011). The high MW kinase-inactive P-TEFb complex contains 7SK RNA (Nguyen *et al.*, 2001; Yang *et al.*, 2001) and several proteins in addition to CDK9/cyclin T1 including the hexamethylene bis-acetamide-inducible protein 1 (HEXIM1) dimer, La-related protein 7 protein (He *et al.*, 2008; Krueger *et al.*, 2008; Markert *et al.*, 2008) and the methyl phosphatase capping enzyme (Jeronimo *et al.*, 2007; Barboric *et al.*, 2009). This P-TEFb complex serves as a source of CDK9/cyclin T1 for recruitment by HIV-1 Tat (Sedore *et al.*, 2007). CDK9/cyclin T1 association with 7SK RNA requires phosphorylation of CDK9 at Thr¹⁸⁶ (Chen *et al.*, 2004; Li *et al.*, 2005). Dephosphorylation of CDK9 on Thr¹⁸⁶ by protein phosphatase-1 (PP1) in stress-induced cells dissociates 7SK RNA and HEXIM1 and activates CDK9/cyclin T1 (Chen *et al.*, 2008). Dephosphorylation of Ser¹⁷⁵ in the T loop of CDK9 by PP1 induces CDK9 activity and activates HIV-1 transcription (Ammosova *et al.*, 2011a). Deregulation of cellular PP1 through expression of the central domain of the nuclear inhibitor of PP1 inhibits HIV-1 transcription and replication (Ammosova *et al.*, 2011b) and also increases CDK9-Ser¹⁷⁵ phosphorylation and inhibits the enzymic activity of CDK9 (Ammosova *et al.*, 2011a). In HIV-1 Tat, a short protein sequence (Val³⁶ to Phe³⁸, also referred to as the RVxF sequence) interacts with PP1 and facilitates translocation of PP1 to the nucleus (Ammosova *et al.*, 2005).

We recently developed low MW compounds targeting PP1 that were modelled to fit this RVxF-accommodating groove of PP1 (Ammosova *et al.*, 2012). We virtually screened 300 000

compounds and of these, selected the best 1000. We then experimentally screened these 1000 compounds and selected one hit compound, 1H4 (see Figure 1 and Table 1), that inhibited HIV-1 transcription and replication at non-cytotoxic concentrations, with an IC₅₀ value of 10 µM (Ammosova *et al.*, 2012). The compound 1H4 prevented PP1-mediated dephosphorylation of a substrate peptide containing an RVxF sequence *in vitro*, disrupted the association of PP1 with Tat in cultured cells and prevented the translocation of PP1 to the nucleus (Ammosova *et al.*, 2012).

Here we report further development of the approach to HIV-1 inhibition through targeting PP1. We applied an iterative procedure (design-synthesis-evaluation) to the modification of the structure of 1H4 in order to improve inhibition of HIV-1 replication without increasing cellular toxicity. Through the sequential analysis of several libraries, we obtained HIV-1-inhibitory compounds with higher inhibitory properties and lower toxicity than the initial 1H4 compound. We also confirmed the mechanism of action of the PP1-targeting molecules by determining the affinity of binding of these molecules to PP1, by analysing their effect on PP1 activity, on disruption of PP1 binding to Tat and on shuttling of PP1 to the nucleus.

Methods

Cells

CEM-HIV-1 (LTR) GFP cells, HIV-1 LTR-LacZ reporter (Kimpton and Emerman, 1992) and pNL4-3.Luc.RE⁻ (Gervais *et al.*, 1997) were obtained from the NIH AIDS Research and Reference Reagent Program (Germantown, MD, USA). Peripheral blood mononuclear cells (PBMCs) were purchased from Astarte Biologics (Redmond, WA, USA).

Design of the 1H4-derived library

The first library was based on substructure search from Enamine stock collection. Instant JChem 5.3.4, from ChemAxon (<http://www.chemaxon.com>) was used for structure compound database management and search. The previously suggested model of interaction between PP1 and the compound 1H4 (Ammosova *et al.*, 2012) implies that the quinoline moiety of 1H4 binds in the RVxF-accommodating hydrophobic groove. To cover a wide variety of derivatives of 1H4, we selected compounds that fill the search pattern:

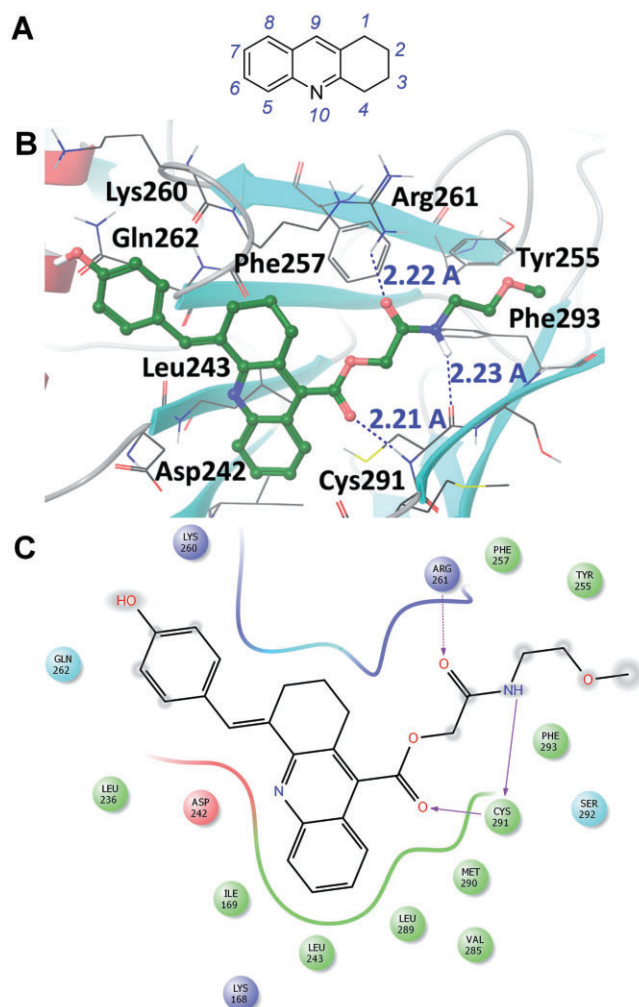
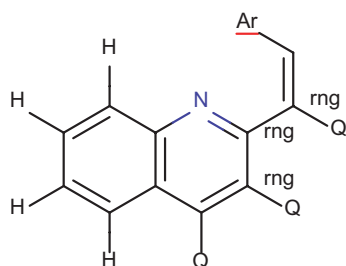


Figure 1

Model of the interactions of 1H4 with the RVxF binding cavity of PP1. (A) Numbering of the tetrahydroacridine analogues. (B) Atomic representation of 1H4 docked into the RVxF-binding cavity. (C) Contact map for 1H4. Tetrahydroacridine core and substitutions at position 4 of 1H4 are involved in extensive van der Waals contacts. The flexible tail at position 9 of 1H4 forms three hydrogen bonds with backbone atoms and the guanidine group of Arg²⁶¹.M

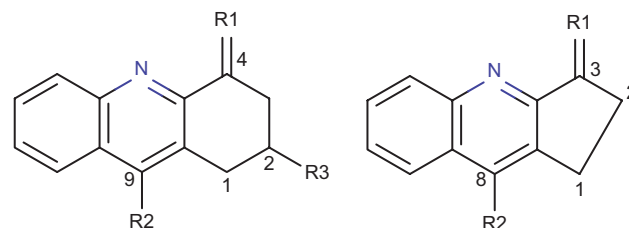


Ar – an aromatic ring

Q – a heavy atom

rng – exocyclic rings and substituents covalently bound to the central quinoline ring

Substitutions in the phenyl ring were not allowed. The search led to the identification of substituted acridines (Scaffold A) and 2,3-dihydro1*H*-cyclopenta[*b*]quinolines (Scaffold B). The selected compounds had either two or three points of variation (R₁, R₂ and R₃).



Scaffold A

Scaffold B

The full list of acridine derivatives of the compound 1H4 can be downloaded (Supporting Information Table S1).

The design of our second library was based on the *in vitro* screening data obtained from the first screen and the analysis of the binding model of the compound 1H4 to PP1. The synthesis of acridine derivatives was performed at Enamine facilities (Kiev, Ukraine) using standard protocols. A total of nine compounds were synthesized for the second iteration.

Tat-induced HIV-1 transcription

CEM-GFP cells were infected with AdTat and GFP fluorescence was measured as described (Ammosova *et al.*, 2012). The 293T cells were co-transfected with a Tat-expressing vector and vectors containing HIV-1 LTR-*Lac Z* and CMV-EGFP. Then HIV-1 transcription was analysed as described (Ammosova *et al.*, 2012). CEM T-cells and PBMCs were infected with VSVG-pseudotyped pNL4-3.Luc.R-E-virus (HIV-1 Luc) prepared as previously described (Debebe *et al.*, 2011). A subset of the PBMCs were activated by treating them with 2.5 µg mL⁻¹ phorbol 12-myristate 13-acetate for 24 h and then with 50 units·mL⁻¹ IL-2 for another 24 h before infecting with HIV-1 Luc. Cells were lysed using the Lucite buffer system (Perkin Elmer, Shelton, CT, USA) and luciferase activity measured.

Cell viability assays

Cytotoxicity was determined with propidium iodide and viability with Trypan blue and calcein AM using an automated cell counter (Nexcelcom, Lawrence, MA, USA). Both procedures were based on previously established protocols (Ammosova *et al.*, 2012).

HIV-1 inhibition assays

Inhibition of HIV-1 by the indicated compounds was conducted by Reginald Clayton at HIV Integrase Discovery Group, Tibotec. HIV-1 replication was measured as an induction of EGFP protein expression in MT4-LTR-EGFP cells which contained an integrated EGFP construct under the control of the HIV-1 LTR and had been infected with wild-type WT HIV-1 IIIB or the integrase mutants, Q148R and N155H.

pRb dephosphorylation assay

The assay was performed at 30°C for 30 min in 24 µL of kinase assay buffer (50 mM HEPES-KOH, pH 7.9, 10 mM

Table 1

Selected 1H4-derived compounds that inhibited HIV-1 transcription

Compound number	ID	Inhibition of HIV-1 transcription in CEM-GFP cells (IC ₅₀ , µM)	Toxicity in CEM cells (IC ₅₀ , µM)	Inhibition of HIV-1 transcription in 293T cells (IC ₅₀ , µM)
Reference	1H4	10	>25	>10
1	1D4	10	>25	5
2	<i>1D5</i>	<i>10</i>	<i>2</i>	<i>0.1</i>
3	1E6	10	>25	5
4	1G6	5	>25	4
5	1C10	8	>25	>10
6	1D9	15	>25	4
7	<i>1E7</i>	<i>2</i>	<i>16</i>	<i>0.9</i>
8	1D10	8	>25	4
9	2C2	6	>25	4
10	<i>2F2</i>	<i>6</i>	<i>17</i>	<i>0.3</i>
11	2B3	10	>25	6
12	2A5	5	2	0.1
13	2H4	10	>25	>10
14	3B3	12	>25	2

Compounds with the lowest IC₅₀ in 293T cells and the lowest toxicity are shown in italic.

MgCl₂, 2 mM EGTA, 2.5 mM DTT) containing 0.1 µg CDK2/cyclin E, 1 µg of recombinant pRb as a substrate, 200 µM of unlabelled ATP and 5 µCi of [³²P]γ-ATP. CDK2 activity was inhibited by adding the CDK2 inhibitor, roscovitine, into the reaction. Then, 0.2 µL (5 U) of PP1 was added to the reaction mixture, which was supplemented with 1 mM MnCl₂. PP1-inhibiting compounds and microcystin-LR were added as indicated. After incubation at 30°C for 30 min, the reaction was stopped with an SDS-loading buffer. The reaction mixture was resolved on 10% PAGE and the gel was exposed to a phosphor imager screen (Perkin Elmer).

Assay of C-terminal domain of RNA polymerase II (CTD) phosphorylation

This assay was performed at 30°C for 30 min in 24 µL of kinase assay buffer containing recombinant 0.1 µg CDK9/cyclin T1, 2 µg of GST-CTD substrate, 60 µM cold ATP, 5 µCi of [³²P] γ-ATP. Where indicated, 30 µM ARC (a known inhibitor of CDK9), or 3 or 30 µM of either 1H4, compound 7 or compound 10 were used. The reaction was stopped with an SDS-loading buffer, the reaction mixture was resolved on 10% PAGE and the gel was exposed to a phosphor imager screen.

PP1 expression

BL21 (DE3) *Escherichia coli* cells (Invitrogen, Carlsbad, CA, USA) were co-transformed with a vector PP1 7-300, which expresses human PP1α (residues 7–300) and pGR07, which expresses GroEL/GroED chaperones (both gifts from Dr Mathieu Bollen and Monique Beullens, KU Leuven, Belgium). The cells were grown in media supplemented with 1 mM

MnCl₂ at 30°C to an A₆₀₀ ~0.5. Then arabinose (2 g L⁻¹) was added to induce expression of the GroEL/GroES chaperones. When A₆₀₀ ~1 was reached, the cells were transferred to 10°C and PP1 expression was induced with 0.1 mM Isopropyl β-D-1-thiogalactopyranoside for 20 h. Harvested cells were lysed using sonication in a solution containing in 50 mM Tris-HCl (pH 8.0), 5 mM imidazole, 700 mM NaCl, 1 mM MnCl₂, 0.1% Triton X-100 (v/v) and protease inhibitors. His-tagged PP1 was purified using a Ni-NTA IMAC column (Qiagen, Valencia, CA, USA). PP1 was then dialyzed and stored at -70°C in 50 mM Tris-HCl (pH 8.0), 5 mM imidazole, 700 mM NaCl and 1 mM MnCl₂. PP1 activity was then assayed as previously described (Ammosova *et al.*, 2012).

Surface plasmon resonance (SPR)

All SPR measurements were conducted on a Biacore T200 instrument (GE Healthcare, Piscataway, NJ, USA) at 25°C. Recombinant His-tagged PP1 was immobilized on a Ni-NTA sensor chip (GE Healthcare). The two-flow cells of the sensor chip were primed with running buffer (0.01 M HEPES pH 7.4, 0.15 M NaCl, 0.005% v/v surfactant P20, 1% DMSO and 2 mM MnCl₂) and loaded with 0.5 mM NiCl₂ at a flow rate of 10 µL min⁻¹ for 180 s. After NiCl₂ injection, both flow cells were washed twice with the running buffer at flow rate of 100 µL min⁻¹ for 40 s. PP1 was diluted with the running buffer to a concentration of 200 nM and was then passed over the second flow cell of the sensor chip at a flow rate of 5 µL min⁻¹. The final amount of PP1 immobilized on the surface was 3500 RU. The first flow cell was only loaded with Ni²⁺ and was used as a reference for non-specific background

binding during the experiment. For binding and kinetics experiments, all compounds were diluted in the running buffer, at 50, 25, 12.5, 6.25, 3.125, 1.56 and 0 μM and were passed over the two-flow cells at a flow rate of 100 $\mu\text{L min}^{-1}$ for 60 s. The number of response units was recorded after the subtraction of the reference flow cell's value (Fc2-1). Three repetitions were performed for each injection. Data were analysed using the BiaEvaluation software of Biacore (GE Healthcare) with a 1:1 binding model.

Toxicity and pharmacokinetic (PK) analysis in mice

All animal care and experimental procedures were approved by the George Mason University (toxicity studies) and Children's Research Institute (PK studies) Animal Care and Use Committees. All studies involving animals are reported in accordance with the ARRIVE guidelines for reporting experiments involving animals (<B50>Kilkenny *et al.*, 2010</C>; <B51>McGrath *et al.*, 2010</C>). A total of 18 animals were used in the experiments described here.

Toxicity of the compound 7c was assessed in 8-week-old mice with deletion of the IFN- α/β receptor (IFNR $^{-/-}$). Female mice IFNR $^{-/-}$ mice with C57Bl/6 background ($n = 9$) were obtained from Jackson Laboratory. The mice were injected i.p. daily with DMSO or one of two concentrations of compound 7c (10 or 25 mg kg^{-1}) for up to 10 days ($n = 3$ per treated group). Each day, the mice were weighed, as a group, and monitored for any signs of stress. All animals survived the 10 day treatment.

For PK studies, FVB/N male mice (8 weeks old, 25–30 g) were purchased from Jackson Laboratory (Bar Harbor, ME, USA) and housed in a pathogen-free environment. Mice ($n = 6$ mice per experimental group and $n = 3$ per control group) were injected i.p. with compound 7c (25 mg kg^{-1}) dissolved in 80% DMSO or, in the case of the control group, with 80% DMSO. Blood samples (150 μL) from three mice injected with compound 7c (half of the experimental group) were taken at 15 min, 30 min, 1 h, 3.5 h, 6 h, 24 h and 48 h after the treatment. Mouse plasma (10 μL) was diluted with 10 μL of PBS and mixed. Protein was precipitated with the addition of 2.6 μL of 100% trichloroacetic acid for 15 min on ice. The reaction mixture was centrifuged at 12 000 g for 10 min at 4°C and the supernatants (10 μL) were collected. The supernatants were vacuum-dried, dissolved in 10 μL of 0.1% trifluoroacetic acid (TFA) and loaded into a zip-tip. The zip tips were eluted with a solution containing 80% acetonitrile (ACN) and 0.1% TFA, and then the eluates were vacuum-dried and dissolved in 40 μL of 0.1% TFA for LC-MS analysis. To analyse the stability of compound 7c in murine plasma, the compound was dissolved in the plasma and incubated for 1 min, 15 min or 2 h. The compound was extracted as described earlier and subjected to the LC-MS analysis as described below.

LC-MS analysis of compound 7c

The compound 7c, either in purified form or isolated from murine plasma, as described earlier, was separated by reversed-phase liquid chromatography (HPLC), using microcapillary C18 column, coupled in line with a tandem mass spectrometer Thermo LTQ Orbitrap XL (West Palm Beach, FL,

USA). Each sample (10 μL) was injected on the C18 nano-column and separated in a 0.1–80% ACN gradient containing 0.1% TFA, with a run time of 35 min. The mass spectrometer was operated in a data-dependent MS/MS mode using normalized collision-induced dissociation energy of 35%.

Data analysis

Results are expressed as means with SD. Differences between any two groups were compared using the Student's *t*-test with GraphPad Prism 4.01 software (GraphPad Software, La Jolla, CA, USA).

Materials

Flag-Tat expression vector was as previously described (Ammosova *et al.*, 2006). CDK9/cyclin T1 (Peng *et al.*, 1998) and CDK2/cyclin E (Deng *et al.*, 2002) were purified as described. Recombinant PP1 α was obtained from New England Biolabs (Ipswich, MA, USA). Human retinoblastoma protein-derived peptide (pRb) was obtained from Sigma (Atlanta, GA, USA). Glutathione S-transferase (GST)-fused CTD was purified as described (Peterson *et al.*, 1992). Histone H1 was obtained from Upstate Cell Signaling Solutions (Charlottesville, VA, USA). ARC (4-amino-6-hydrazino-7- β -D-ribofuranosyl-7H-pyrrolo[2,3-d]-pyrimidine-5-carboxamide) was a gift from Dr A. Gartel. Anti-Flag antibodies and anti-tubulin antibodies were obtained from Sigma. Protein G agarose was obtained from Upstate (Lake Placid, NY, USA). Antibodies against PP1 α were obtained from EMD Chemicals (Gibbstown, NJ, USA). Anti-GFP antibodies were obtained from Santa Cruz Biotechnology (Dallas, TX, USA).

Results

First round modification of the 1H4 structure

We designed various 1H4 analogues to improve the HIV-1 inhibitory activity and reduce cytotoxicity of this lead compound. We used a model of the 1H4 compound bound to the RVxF-accommodating cavity of PP1 (Ammosova *et al.*, 2012) (Figure 1). In this model, modifications of the tetrahydroacridine core at positions 4 and 9 (see numbering in Figure 1, panel A) and the associated conformations contributed significantly to the binding (Figure 1, panels B and C) (see also Structure–activity relationship section for additional details). The first round of modifications was aimed at the exploration of the chemical space around the core of 1H4 (1,2,3,4-tetrahydroacridine). We searched the Enamine stock collection for all existing tetrahydroacridine structures related to 1H4 and obtained a cumulative library of 143 compounds (see Supporting Information Table S1, compounds 1–143). These compounds were evaluated for the inhibition of Tat-dependent HIV-1 transcription using a previously described CEM T-cell line. This cell line contained integrated GFP under the control of an HIV-1 promoter (CEM-GFP cells). CEM-GFP cells were infected with an adenovirus that expresses the HIV-1 Tat activator protein (Ad-Tat) (Nekhai *et al.*, 2007). Infected CEM-GFP cells were incubated with 25 μM of each compound for 48 h. Compounds that inhibited HIV-1 transcription by 50% or higher at a concentration of 25 μM were chosen for further analysis. A total of 43 compounds were

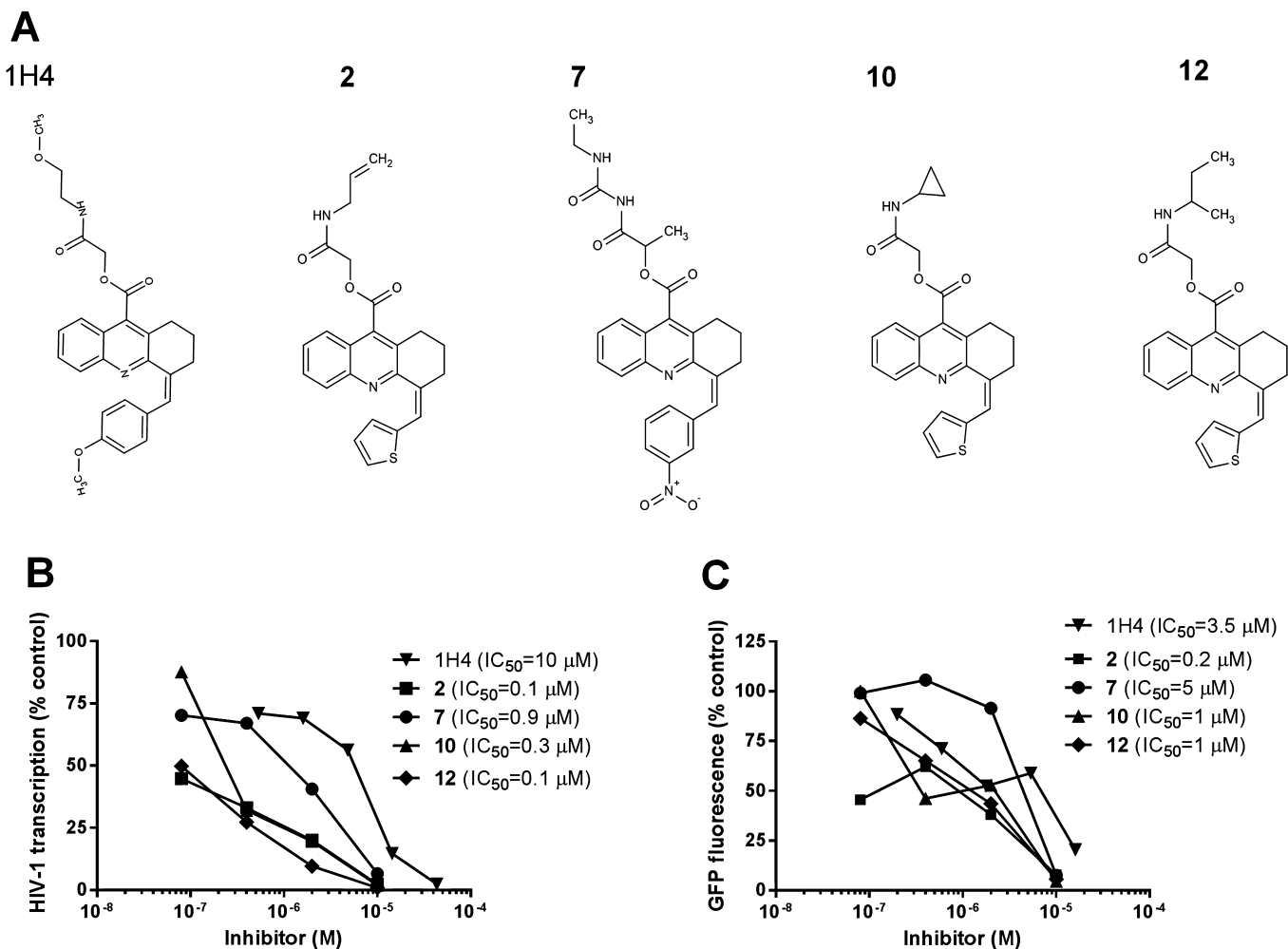


Figure 2

Inhibition of HIV-1 transcription by 1H4 analogues from the first round of optimization. (A) Chemical structures of compounds. (B, C) Inhibition of HIV-1 and CMV transcription. The 293T cells were transfected with HIV-1 LTR-LacZ, EGFP expression vectors and Tat-expressing vectors and treated with the indicated concentrations of compounds. Twenty-four hours after the transfection, the cells were lysed and analysed for β -galactosidase activity (B) or EGFP fluorescence (C). Results shown are from one experiment of two performed.

selected and analysed at different concentrations to determine the IC_{50} values for the inhibition of HIV-1 transcription and also to monitor toxicity. We identified 14 compounds that inhibited HIV-1 transcription in CEM-GFP cells with IC_{50} values below 25 μ M (Table 1). These 14 compounds were evaluated further to determine whether HIV-1 LTR-directed transcription was inhibited in 293T cells transfected with a Tat-expressing vector and an HIV-1 LTR-LacZ reporter. Compounds 2, 7, 10 and 12 (Figure 2A) inhibited HIV-1 transcription with IC_{50} values below 1 μ M (Figure 2B and Table 1, in *italic*). However, only compound 7 showed a promising toxicity profile (Table 1) and a higher specificity when analysed for the inhibition of unrelated CMV-promoter driven GFP (Figure 2C). The previously described 1H4 compound was found to be a less potent inhibitor of HIV-1 transcription (Figure 2B) and showed less specificity than compound 7 (Figure 2C). We further analysed the effect of compound 7 on HIV-1 by looking at both the compound's inhibition of

Table 2

Inhibition of wild-type (IIIB) and mutant HIV-1

Compound number	ID	HIV-1 IIIB (IC_{50} , μ M)	HIV-1 Q148R (IC_{50} , μ M)	HIV-1 N155H (IC_{50} , μ M)
Reference	1H4	9.4	4.7	8
Control	1G3	37	42	59
7	1E7	2.5	1.5	3.2

mutated HIV-1 viruses (Table 2). Both compound 7 and 1H4 inhibited HIV-1 replication, but compound 7 consistently showed significantly greater inhibition than 1H4 with IC_{50} values that were at least 2.5 times lower (Table 2). Thus, we chose compound 7 for further analysis and optimization.

Compound 7 prevents the interaction of HIV-1 Tat with PP1 and the shuttling of PP1 to the nucleus

We previously reported that 1H4 interfered with the binding of the HIV-1 Tat protein to PP1 (Ammosova *et al.*, 2012). To analyse whether compound 7 disrupted the interaction of Tat with PP1, we expressed Flag-Tat in 293T cells and treated the cells with either 10 or 30 μ M concentrations of either 1H4, compound 7 or compound 10 (Figure 3A). Flag-Tat was immunoprecipitated with anti-Flag antibodies and co-precipitated endogenous PP1 α was detected with anti-PP1 antibodies (Figure 3A, lane 2). At 30 μ M, compound 7 decreased the amount of co-precipitated endogenous PP1 α by threefold (Figure 3A, lane 8), whereas compound 10 reduced the amount of co-precipitated PP1 α only by 1.7-fold (Figure 3A, lane 6) and 1H4 had no effect on the amount of co-precipitated PP1 α (Figure 3A, lanes 3 and 4). To analyse the effect of compound 7 on the shuttling of PP1 α between the cytoplasm and the nucleus, we measured the fluorescence of PP1 α -EGFP in nuclear and cytoplasmic fractions of 293T cells. These cells were transfected with either Tat and the PP1 α -EGFP expression vector or only the PP1 α -EGFP expression vector and then treated with either compound 7, compound 1H4 and or an inactive compound (control). The cytoplasmic and nuclear fractions were separated, as previously described (Ammosova *et al.*, 2012). Analysis of EGFP fluorescence showed that nuclear PP1 α -EGFP was decreased by 2.4-fold in 1H4-treated cells and 1.7-fold in compound 7-treated cells (Figure 3B, lanes 3 to 5), consistent with the idea that compound 7 interferes with the binding of Tat to PP1. In contrast, 1H4 had no effect on PP1 distribution and compound 7 decreased nuclear PP1 by 1.15-fold in the absence of Tat (Figure 3C). Together, these results indicated that the compound 7 may affect HIV-1 transcription by interfering with the interaction of HIV-1 Tat with PP1 and by preventing the shuttling of PP1 to the nucleus.

Compound 7 does not have a significant effect on PP1 and CDK9 activities *in vitro*

To determine whether compound 7 had an effect on PP1 activity *in vitro*, we analysed the dephosphorylation of pRb that was phosphorylated prior to the addition of the phosphatase. The action of PP1 on the [³²P]-phosphorylated pRb peptide resulted in a fourfold loss of phosphorylation (Figure 3D, lanes 1 and 2). Inhibition of PP1 activity by microcystin, a competitive PP1 inhibitor, decreased pRb dephosphorylation by 72% (Figure 3D, compare lanes 2 and 6). The effect of microcystin confirmed that the dephosphorylation effect was due to PP1. Compounds 7 and 10 each reduced pRb dephosphorylation by 15%, a relatively small inhibitory effect (Figure 3D, lanes 4 and 5). The compound 1H4 had an even smaller effect, reducing pRb dephosphorylation by only 4% (Figure 3D, lane 3).

We next analysed whether compound 7 inhibited the activity of CDK9, which is critical for HIV-1 transcription. We incubated recombinant CDK9/cyclin T1 with recombinant GST-CTD as a substrate, either with or without the addition of either 1H4, compound 7 or compound 10 (Figure 3E). Addition of 30 μ M ARC, previously shown to inhibit CDK9 activity (Radhakrishnan and Gartel, 2006) and HIV-1 transcription

(Nekhai *et al.*, 2007), to our assays inhibited CDK9 activity reducing GST-CTD phosphorylation by 27%. Compounds 7 and 10 (tested at 3 or 30 μ M concentrations) each reduced CTD phosphorylation by less than 7%. Thus compound 7 did not directly inhibit PP1 or CDK9 activity, but did affect PP1 shuttling and prevented the interaction of PP1 with Tat in cultured cells.

Second round modification of compound 7

While compound 7 showed improved HIV-1 inhibition, its cytotoxicity remained relatively high, compared with that of 1H4 (IC_{50} = 16 μ M, Table 3). Based on the structure–activity relationship data from the first round of modification (see Structure–activity relationship section), we designed and synthesized a second library of 10 compounds. In designing the library, we focused our attention on the following criteria (i) position 4 in the tetrahydroacridine ring must tolerate small aromatic groups; (ii) the saturated ring in the core must be unsubstituted; and (iii) only flexible linear linkers enriched with hydrogen bonding functionalities are acceptable at position 9. Corresponding compounds were synthesized *de novo* (see Figure 4A for the synthesis scheme) and were analysed for the inhibition of single round HIV-1 replication in CEM cells infected with HIV-1 Luc virus. Two compounds, compound 7c and compound 7d inhibited HIV-1 (Table 3, see compounds 7a–7g; and Figure 4, panels B and C) with IC_{50} values similar to the IC_{50} of the parental compound 7. While compound 7c was not cytotoxic at a concentration of 300 μ M, the parental compound 7 decreased viability of HIV-1 infected CEM T-cells with IC_{50} = 16 μ M. Compound 7d also decreased viability with IC_{50} = 26 μ M (Figure 4D). Analysis of HIV-1 infection in primary PBMCs showed that compound 7c inhibited HIV-1 with IC_{50} = 4 μ M and caused less than a twofold decrease in viability at a concentration of 100 μ M (Figure 4E).

Next, we analysed the *in vivo* toxicity of compound 7c in mice. Eight-week-old IFN α –/– mice were injected i.p. daily with either DMSO or one of two doses of compound 7c (10 or 25 mg kg^{–1}) for up to 10 days. IFN α –/– mice were chosen for these experiments because they are immunocompromised by the deletion in the receptor for IFN α and β , and therefore are very useful models for toxicity testing. The mice were observed daily for any signs of stress and weighed. They did not display any signs of toxicity or stress, such as ruffled fur or lethargy. No significant changes were observed in the mice treated with compound 7c over the course of the study (Figure 4F). Interestingly, the mice gained weight over the 10 day period. In addition, on days 2–10 of the study, mice treated with compound 7c weighed more than those treated with DMSO (the control group). These results indicate that compound 7c does not display any overt toxicity *in vivo*.

PK analysis of compound 7c in mice

Next we characterized PK of compound 7c in mice. We detected compound 7c by LC-MS with C18 column prepared in-house and linked to the LTQ Orbitrap mass spectrometer. Analysis of compound 7c (molecular weight = 503.2 g mole^{–1}) showed the presence of a major [M + H]⁺ peak, corresponding to a molecular weight of 504.22 Da (Figure 5A). This value is consistent with the molecular weight of compound 7c when

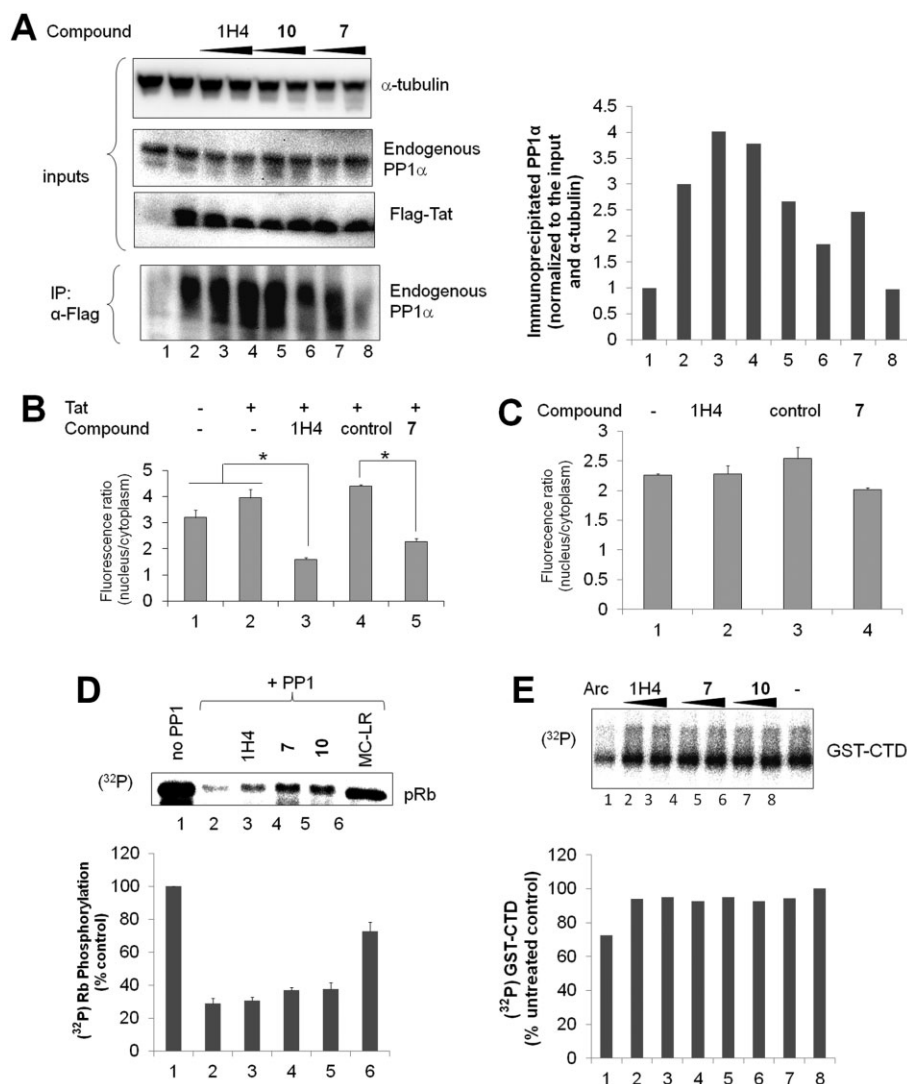


Figure 3

Compound 7 affects the interaction of PP1 with Tat as well as its translocation to the nucleus but has no effect on PP1 or CDK9 activity. (A) 1H4 prevents the interaction of Tat with PP1 in cultured cells. HEK293T cells were transfected with Flag-tagged Tat. Flag-Tat was immunoprecipitated with anti-Flag antibodies and co-precipitated PP1 was detected with antibodies that recognize PP1 α . The α -Flag antibodies were used to detect Tat. Lane 1, control cells; lanes 2–8 cells transfected with Flag-Tat. Lanes 3 and 4, cells treated with 1H4 at 2 and 10 μ M respectively; lanes 5 and 6, cells treated with compound 10 at 2 and 10 μ M respectively; and lanes 7 and 8, cells treated with compound 7 at 2 and 10 μ M respectively. Results shown are from one experiment of two performed. (B, C). Compound 7 disrupts translocation of PP1 to the nucleus. HEK293T cells were transfected with PP1 α -EGFP and Tat expression vectors (B) or only PP1 α -EGFP vector (C) and then treated with the indicated compounds for 24 h. The cells were lysed in low salt buffer and the cytoplasmic extract was separated from the nuclear material by centrifugation. Fluorescence was measured in the nuclear and cytoplasmic fractions using a Perkin-Elmer Luminoscan spectrofluorimeter. Data shown are means (with SD) from three experiments. * $P < 0.01$; significantly different as shown. (D) Compound 7 has no significant effect on PP1-mediated dephosphorylation of pRb. The kinase assay was performed using recombinant CDK2, with recombinant pRb and [32 P] γ -ATP as substrates. CDK2 was inhibited with 2.5 μ M roscovitine. Then 30 μ M of either 1H4 (lane 3), compound 7 (lane 4), or compound 10 (lane 5) or 50 nM of microcystin-LR (lane 6) was added. Each reaction was then supplemented with 1 mM MnCl₂ and 5 U of recombinant PP1 (lanes 2 through 6). Lane 1 was a positive pRb phosphorylation control to which PP1 was not added. Reactions were resolved on 10% SDS-PAGE and quantified using the Phosphor Imager. Lower panel shows means (with SD) from three experiments. (E) Compound 7 has no effect on the enzymic activity of CDK9. Kinase assay was performed using recombinant CDK9, with the C-terminal domain of RNA polymerase II (CTD) and [32 P] γ -ATP as substrates. Lane 8, phosphorylation of CTD by recombinant CDK9/cyclin T1. Lane 1, 30 μ M CDK9 inhibitor (ARC) was added. Lanes 2 and 3, compound 1H4 was added at 3 and 30 μ M respectively; lanes 4 and 5, compound 7 was added at 3 and 30 μ M respectively; and lanes 6 and 7, compound 10 was added at 3 and 30 μ M respectively. Reactions were resolved on 10% SDS-PAGE and quantified using the Phosphor Imager. Results shown are from one experiment of two performed.

Table 3

Structure activity relationship of 1E7 and its derivatives

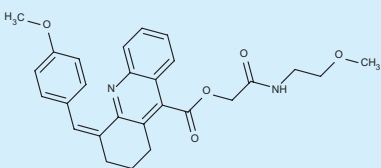
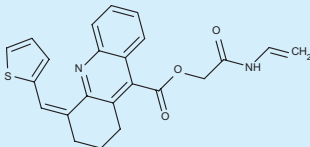
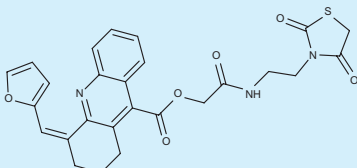
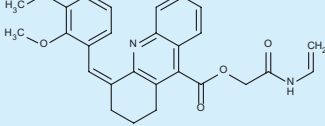
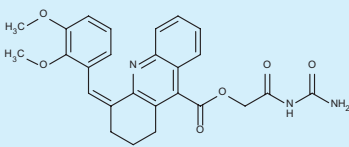
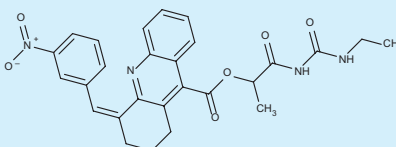
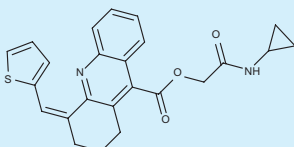
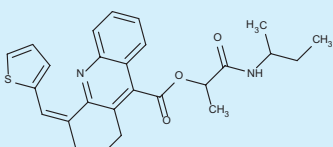
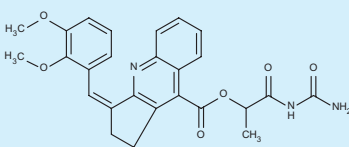
Compound number	ID	Structure	Inhibition IC ₅₀ , CEM T-cells, μ M	Inhibition IC ₅₀ , 293T cells, μ M	Toxicity IC ₅₀ , μ M
		Iteration 1			
	Reference (1H4)		10	5	100
2	1D5		10	0.1	2
3	1E6		1	5	>30
4	1G6		5	4	>30
6	1D9		15	4	>30
7	1E7		2	0.9	10
10	2F2		6	0.2	17
12	2A5		5	0.1	26
14	3B3		12	2	>30

Table 3

Continued

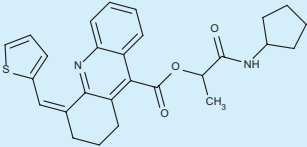
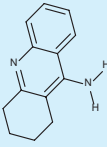
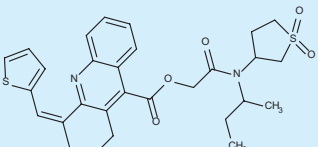
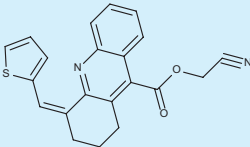
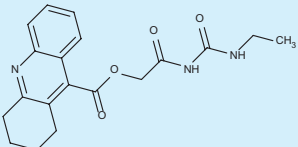
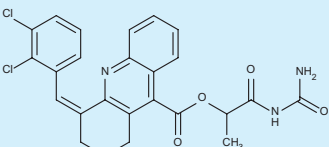
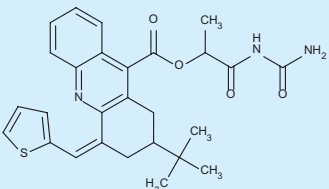
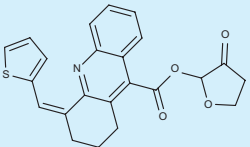
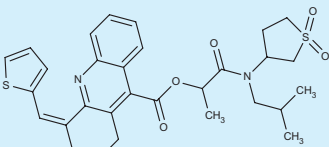
Compound number	ID	Structure	Inhibition IC ₅₀ , CEM T-cells, μ M	Inhibition IC ₅₀ , 293T cells, μ M	Toxicity IC ₅₀ , μ M
15	3A2		ND	10	ND
16	3A7		NA	NA	ND
17	1B10		>50	ND	ND
18	3F8		NA	NA	ND
19	3G6		NA	NA	ND
20	3C2		NA	NA	ND
21	3A3		NA	NA	ND
22	3G8		NA	NA	ND
23	3C10		>50	ND	ND

Table 3

Continued

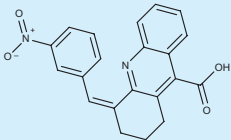
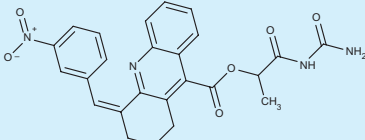
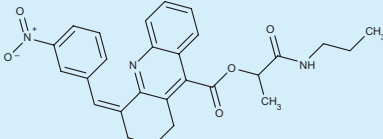
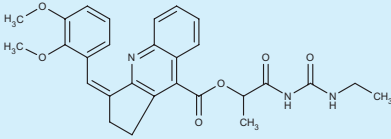
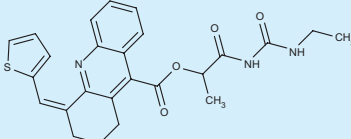
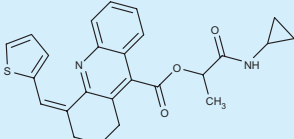
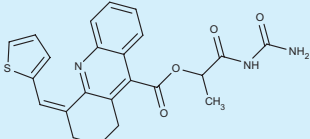
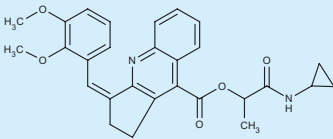
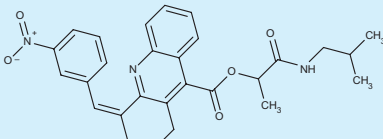
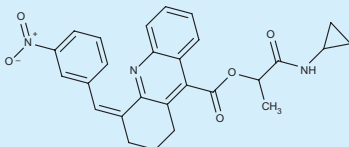
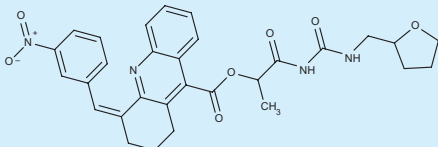
Compound number	ID	Structure	Inhibition IC ₅₀ , CEM T-cells, μ M	Inhibition IC ₅₀ , 293T cells, μ M	Toxicity IC ₅₀ , μ M
24	3G7		NA	NA	ND
Iteration 2					
7a	1E7-01		8	ND	>30
7b	1E7-02		8	ND	>30
7c	1E7-03		2	ND	>300
7d	1E7-04		3	ND	7
7e	1E7-05		>10	ND	>30
7f	1E7-06		>10	ND	>30
7g	1E7-07		activation	ND	>30
7h	1E7-08		>10	ND	>30

Table 3

Continued

Compound number	ID	Structure	Inhibition IC ₅₀ , CEM T-cells, μ M	Inhibition IC ₅₀ , 293T cells, μ M	Toxicity IC ₅₀ , μ M
7i	1E7-09		8	ND	>30
7j	1E7-10		>10	ND	>30

The original compound, 1H4, is placed in the beginning of the table as a reference.
NA, not active; ND, not determined.

a hydrogen cation (H^+) has been added (503 Da). However, when we analysed compound 7c in mouse plasma, we detected a major peak of 557.41 Da (Figure 5B). The incubation of 7c with murine plasma led to facile and irreversible conversion of the 504.22 Da peak into the new 557.41 Da peak. This finding suggests that compound 7c underwent a facile transformation in murine plasma. (Figure 5C). We observed a linear response between the amount of compound 7c and the height of the 557.41 Da peak, within a 10–100 μ M range (Figure 5D). Analysis of the plasma concentration of compound 7c showed that a plateau was reached 1 h after i.p. injection, and that the compound was detected for up to 8 h post-injection. We did not detect the compound at 24 or 48 h post-injection. These results suggested that compound 7c had a half-life greater than 8 h and that it was successfully cleared from the circulation 24 h after i.p. injection.

Compound 7c binds to PP1 *in vitro*

We analysed binding of compound 7c to recombinant PP1 using SPR technology with a Biacore T-200 instrument (Figure 6). Recombinant PP1 protein was expressed in *E. coli* cells (see Methods section). PP1 was immobilized on a sensor chip and different concentrations of compound 7c were injected over the surface of the chip. Direct binding of the compound to PP1 was measured in real time and binding affinity was calculated based on a 1:1 binding model. Compound 7c bound to PP1 with a K_D value of 15.0 μ M, showing its ability to interact with PP1 *in vitro* (Figure 6).

Compound 7c affects the shuttling of PP1 to the nucleus

We further investigated the effects of compound 7c on PP1 by analysing PP1 α distribution in live cells. When expressed in HeLa cells, PP1 α -EGFP exhibits a diffuse localization pattern (Figure 6C, panel a). Co-expression of PP1 α -EGFP with HIV-1 Tat led to the localization of PP1 α to the nucleus (Figure 6C, panel b), a result which is in accordance with those of our

previous study (Ammosova *et al.*, 2005). When treated with either compound 7 or compound 7c, the cytoplasmic pool of PP1 α increased (Figure 6C, panels c and d). In contrast, treatment with the inactive compound 7d did not have an effect on the nuclear localization of PP1 in the presence of Tat (Figure 6C, panel e). Thus, compound 7c prevents the shuttling of PP1 α to the nucleus. This effect is similar to that of compound 7 or of the previously described compound 1H4, both of which caused a reduction in nuclear localization of PP1 α (Ammosova *et al.*, 2012).

Structure–activity relationship

The first round of screening was intended to be as a rapid exploration of the chemical space around the previously identified compound 1H4. We used the model of 1H4 bound to the RVxF-accommodating cavity of PP1 (Ammosova *et al.*, 2012) (Figure 1). According to the model, substitution at position 4 in the tetrahydroacridine ring contributes to van der Waals interactions and hydrogen bonding with Lys²⁶⁰ (Figure 1, panels B and C, see proximity of 1H4's phenyl group to PP1's Lys²⁶⁰). In turn, the flexible moiety at position 9 extends along the cleft and forms three hydrogen bonds. At the end of this cleft there are three aromatic residues, Tyr²⁵⁵, Phe²⁵⁷ and Phe²⁹³, all of which can engage in ligand binding through several mechanisms (Bissantz *et al.*, 2010). A wide range of sulfonamides, esters and amides were included in the screening set.

Screening results revealed that substitutions at positions 4 and 9 are both crucial for antiviral activity. Removing or reducing R1 group (Table 3, compound 19), the R2 group (Table 3, compound 24) or both groups (Table 3, compound 16) all yielded inactive compounds. Electron-rich substituent at position 4 appeared to be advantageous for binding (Table 3, compounds 4, 10 and 12). We did not identify any active compounds with a halogen-substituted aryl group in position 4 that could be attributed to the high lipophilicity or low solubility (e.g. Table 3, compound 20). Surprisingly, only linear flexible non-aromatic substitutions with multiple

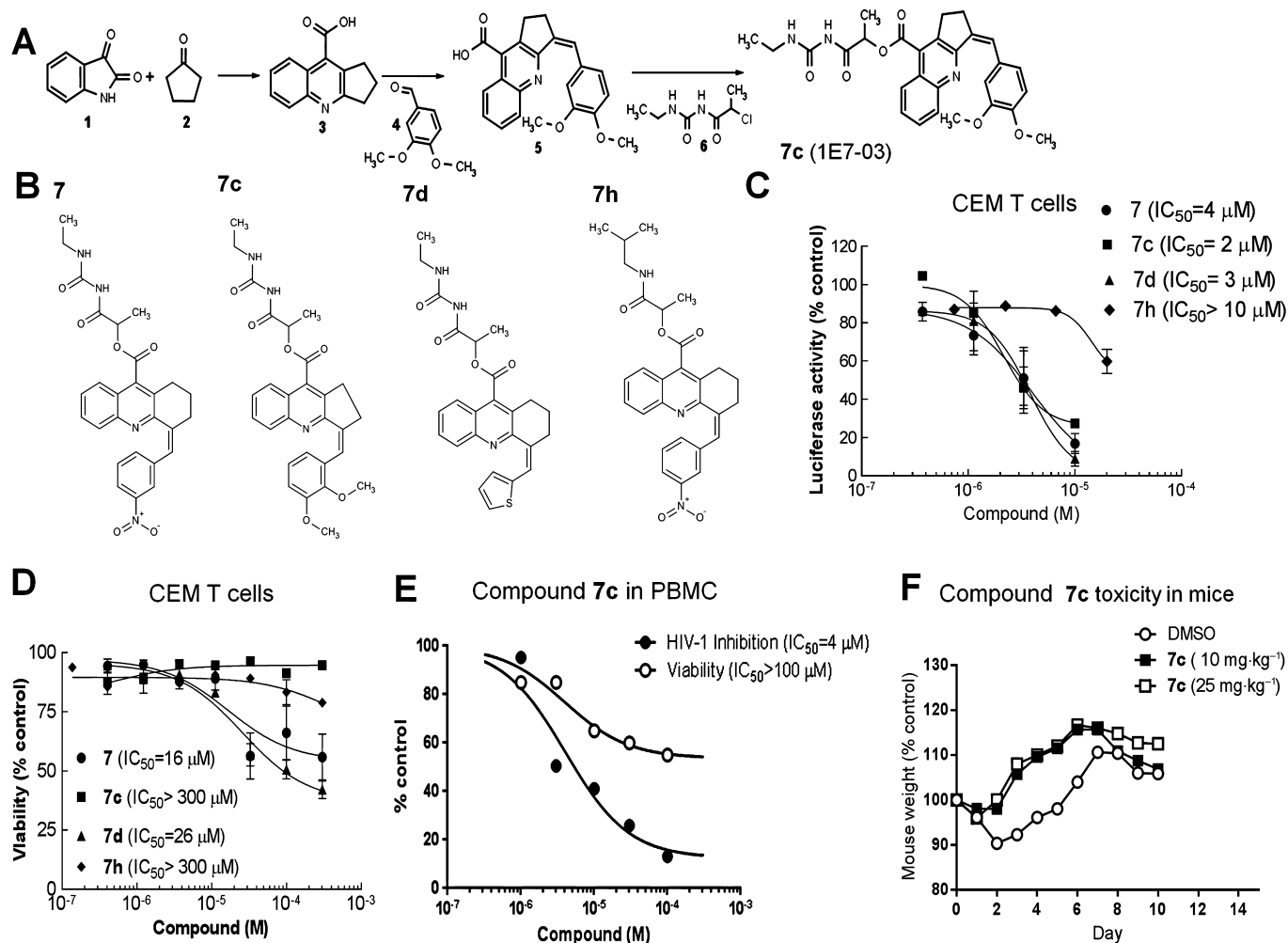


Figure 4

Inhibition of HIV-1 by the analogues of compound 7. (A) Flowchart for the synthesis of compound 7c (1E7-03) (see details in the Methods section). (B) Chemical structures of compounds 7, 7c, 7d and 7h. (C) Inhibition of HIV-1 by compound 7c in CEM T-cells. CEM T-cells were infected with VSVG-pseudotyped HIV-1 virus expressing luciferase for 24 h and then treated with the indicated concentrations of compounds for 24 h. The cells were lysed and luciferase activity was measured. Data shown are means (with SD) from four experiments and were analysed using Prism. (D) Toxicity of compounds in CEM T-cells. CEM T-cells were treated with the indicated concentrations of compound for 24 h. The viability was determined using the Trypan blue exclusion assay. Data shown are means (with SD) from four experiments. (E) Inhibition of HIV-1 in primary PBMCs. PBMCs were treated with phorbol myristate acetate and IL-2 and infected with VSVG-HIV-1 Luc. At 48 h post-infection, the cells were treated with the indicated concentrations of compounds for 24 h. The cells were lysed, using Lucite buffer system and luciferase activity was measured. Data were analysed using Prism. (F) Toxicity of compound 7c in mice. Eight-week-old IFN γ -/- mice were treated daily with either DMSO, 10 mg kg⁻¹ compound 7c or 25 mg kg⁻¹ compound 7c, via i.p. injection ($n = 3$ in each treated group). The mice were treated for 10 days and each treated group weighed daily, as a group. The group body weights are shown as % initial group weights.

hydrogen bonding groups were found among active compounds (Table 3, compounds 2, 3, 4, 6, 10 and 12), which may indicate that hydrogen-bonding interaction is critical for the binding in this region of the RVxF groove. Compound 7 was selected as lead compound from the first round and the second iteration was focused around its structure.

The earlier observations were repeated in the design of the second *de novo* library. The key feature of this set is a flexible tail-like moiety at position 9 that can bind in extended fashion and allow formation of putative hydrogen bonds. Among the synthesized compounds, 7c and 7d, showed activities similar to that of compound 7, but 7c appeared to

be less cytotoxic and therefore was chosen as the final hit compound, as described earlier.

Discussion and conclusions

In the present study, we optimized and screened small, non-peptidic mimics of the 'RVxF'-docking peptide sequence that is found in many PP1-binding regulatory proteins (Hendrickx *et al.*, 2009). In a previous study, we showed that the low MW compound 1H4 disrupted the interaction of HIV-1 Tat's RVxF sequence with PP1 *in vitro* and inhibited HIV-1 transcription

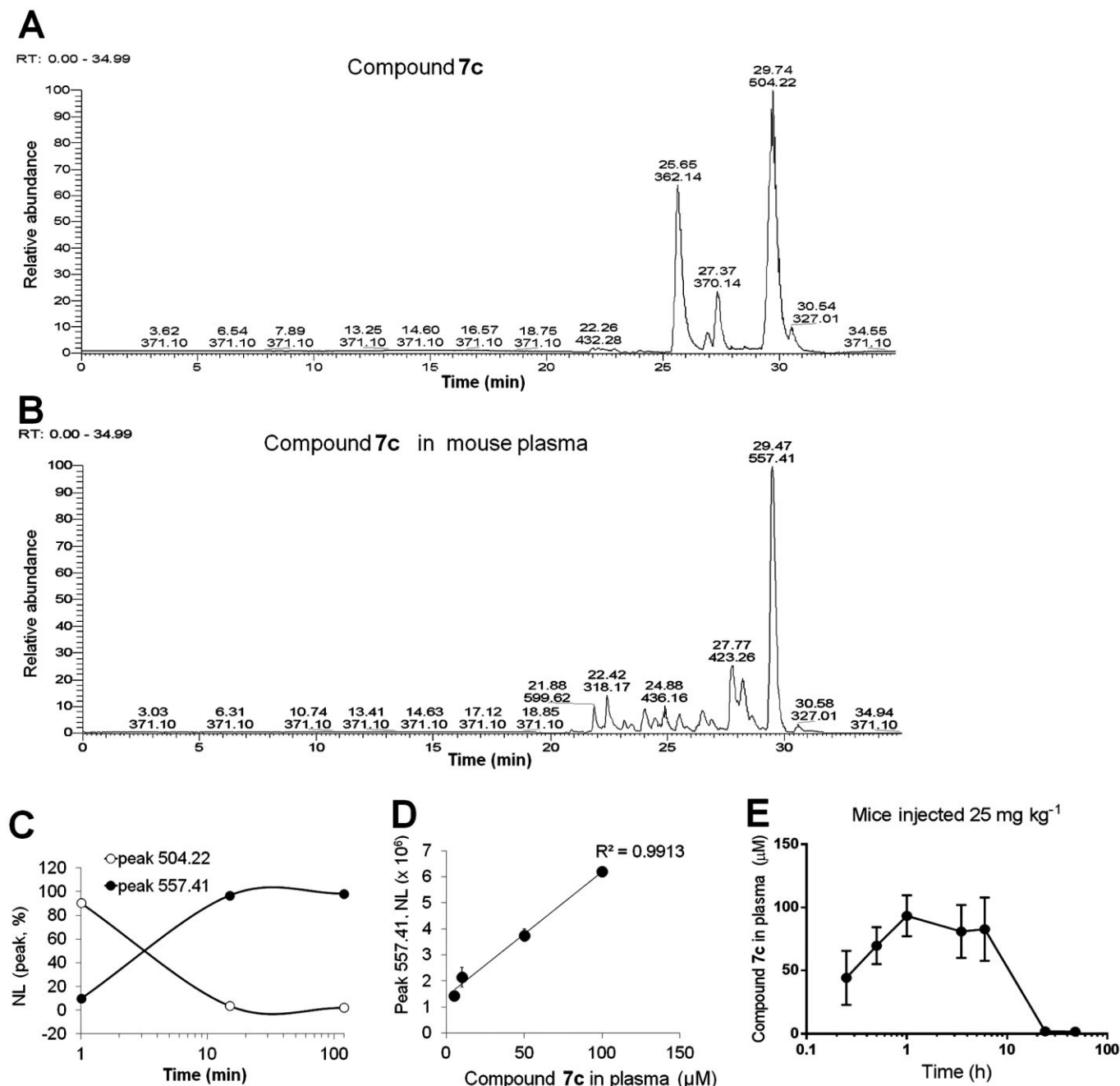


Figure 5

Analysis of the pharmacokinetics (PK) of compound 7c in mice. (A and B) LC-MS analysis of compound 7c. Compound 7c, pure (A) or isolated from murine plasma (B), was resolved on a microcapillary column C18 column coupled to the tandem mass spectrometer Thermo LTQ Orbitrap XL. (C) Conversion of 504.22 Da peak to 557.41 Da peak in murine plasma. Compound 7c was incubated with murine plasma for the indicated amount of time, then extracted (as described in the Methods section), resolved by nano-LC and detected by MS. Samples were measured in triplicate. (D) Linear response of the 557.41 Da peak and the compound 7c in plasma. The indicated amount of compound 7c was incubated with murine plasma for 30 min, then the compound was extracted and resolved by nano-LC and detected by MS. Samples were measured in triplicate. (E) PK analysis of compound 7c in mice. Compound 7c was injected i.p. (25 mg kg⁻¹) and blood was collected as described in the Methods section. The compound was extracted from murine plasma, resolved by nano-LC and detected by MS. Experiments were conducted in triplicate or duplicate as described in the Methods section.

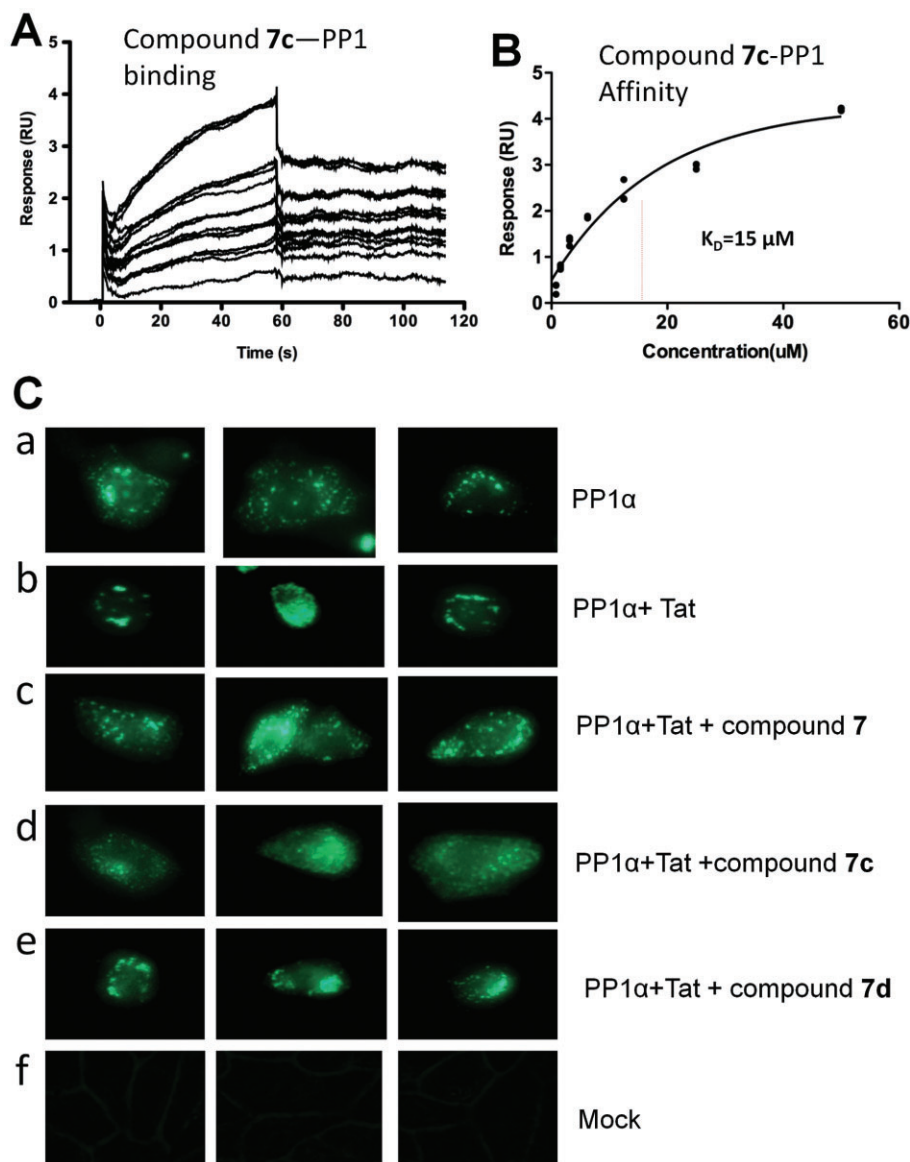


Figure 6

Compound 7c binds to PP1 *in vitro* and disrupts the Tat-mediated translocation of PP1 into the nucleus in cultured cells. (A and B) Direct binding of compound 7c to recombinant PP1 protein. The binding was measured by surface plasmon resonance using a Biacore T-200. Raw data showing binding of 1E7-03 to PP1 protein are presented in panel A. Each line represents a different concentration of compound, all between 0 and 50 μM . The compounds were run in triplicate. The equilibrium dissociation constant (K_D) was calculated, based on a 1:1 binding model, as 15 μM for compound 7c. (B) Each data point represents the binding level shown in panel A from different concentrations of compound 7c measured just before the end of the injection. Vertical dashed lines represent the concentration of ligand that results in a binding level that is 50% of the maximal. (C) Compound 7c disrupts the Tat-mediated translocation of PP1 into the nucleus. HeLa cells were transfected with PP1 α -EGFP (PP1 α) (a), PP1 α -EGFP and WT Flag-Tat (b–e) or mock-transfected (f). The cells were treated with 2 μM of compound 7 (c), 2 μM of compound 7c (d) or 2 μM of compound 7d as a negative control (e) for 18 h. The cells were photographed with a Olympus IX51 with 600X magnification, using a blue filter for EGFP fluorescence or phase contrast.

and replication in cultured cells. In the current study, we have identified a novel compound, 7c which will now be referred to as 1E7-03 (Table 3), that showed no toxicity *in vivo* and that inhibited HIV-1 transcription and replication five times more efficiently than 1H4. The 1E7-03 compound was bioavailable when injected i.p. in mice, and it had a half-life greater than 8 h after the injection. We also significantly extended our previous studies by analysing the binding of

compound 7c to PP1 *in vitro* using the SPR technique. The binding affinity ($K_D = 15 \mu\text{M}$) was in the range of HIV-1 inhibition ($\text{IC}_{50} = 2 \mu\text{M}$), suggesting that the effects of 1E7-03 were caused by its binding to PP1. Also, 1E7-03 prevented the shuttling of PP1 to the nucleus facilitated by HIV-1 Tat. This observation parallels our previous finding, which was that 1H4 inhibits the shuttling of PP1 to the nucleus. This study identifies an optimized hit compound, 1E7-03, which is

suitable for further modifications and animal toxicity testing. Furthermore, our study demonstrates that inhibition of HIV-1 transcription can be achieved by the targeting of PP1.

Our recent studies focused on the role of CDK9 phosphorylation in HIV-1 transcription. Specifically, we investigated the role of CDK9 residues either located within the T-loop, such as Ser¹⁷⁵ and Thr¹⁸⁶, or located in a loop adjacent to the T-loop, such as Ser⁹⁰ (see Nekhai *et al.*, 2014). Phosphorylation of CDK9 at Thr¹⁸⁶ is required for the enzymic activity of CDK9 (Chen *et al.*, 2004; Li *et al.*, 2005) and also facilitates the association of CDK9/cyclin T1 with 7SK RNA snRNP (Chen *et al.*, 2004; Li *et al.*, 2005; Kohoutek, 2009). CDK9-Thr¹⁸⁶ is phosphorylated by CDK7/cyclin H (Larochelle *et al.*, 2012). Phosphorylation of CDK9-Ser¹⁷⁵ allowed better binding of BRD4, a transcription regulator that competes with HIV-1 Tat for CDK9/cyclin T1 (Yang *et al.*, 2005). We demonstrated that inhibition of PP1 by okadaic acid led to an exclusive phosphorylation of CDK9-Ser¹⁷⁵ *in vivo* (Ammosova *et al.*, 2011a). The CDK9 S175A mutant was enzymically active and induced HIV-1 transcription suggesting that PP1 may induce HIV-1 transcription by dephosphorylating CDK9. Recently, induction of CDK9-Ser¹⁷⁵ phosphorylation was reported in activated T-cells with the suggestion that this phosphorylation played a role in HIV-1 viral reactivation in latent cells (Mbonye *et al.*, 2013). We also recently reported the phosphorylation of CDK9-Ser⁹⁰ by CDK2, a process that stimulated HIV-1 transcription (Breuer *et al.*, 2012).

Our recent development of PP1-targeted low MW compounds, such as 1H4 (Ammosova *et al.*, 2012) and now 1E7-03, has served as a proof-of-principle for the design of PP1-targeting compounds to treat HIV-1 transcription. As reported here, 1E7-03 which is an extension of our previous study of 1H4, exhibited direct interaction with PP1. Our study demonstrated that HIV-1 could be inhibited by a non-peptidic, low MW compound that functionally mimics the PP1-binding peptide RVxF. 1H4 and its derivative, 1E7-03, are the first examples of low MW compounds that interact with PP1 and affect HIV-1 transcription. Our study points to PP1 as a new drug target for novel therapeutic agents for retroviral infections.

Acknowledgements

This project was supported by NIH Research Grants 1SC1GM082325 (to S. N.), 1P50HL118006 (to S. N.), District of Columbia Developmental Center for AIDS Research (P30AI087714 to S. N. and A. Ü.), RCMi-NIH 2G12RR003048 from the Research Centers in Minority Institutions (RCMI) Program (Division of Research Infrastructure, National Center for Research Resources, NIH to S. N.) and U19 AI109664-01 (to S. N.). Biacore experiments were carried out at the Genomics and Epigenomics Shared Resource of Lombardi Comprehensive Cancer Center at Georgetown University, which is supported by CCSG Grant P30 CA051008-16. This project was also supported by Civilian Research and Development Foundation grant UKB2-2927-KV-07 (to S. N. and D. K.). The authors thank Dr Marina Jerebtsova and Dr Patricio Ray (Children's National Medical Center, Washington, DC, USA) for the gift of Ad-Tat. The authors also thank Dr Mathieu Bollen and Dr Monique Beullens for the gift of

PP1 and GroEL/GroES chaperon bacterial expression vectors. Dr Michael Emmerman (Fred Hutchinson Cancer Institute, Seattle, WA, USA) is acknowledged for the HIV-1 LTR-*LacZ* expression vector. We thank the NIH AIDS Research and Reference Reagent Program for the pHEF-VSVG expression vector (courtesy of Dr Lung-Ji Chang) and for pNL4-3.Luc.RE⁺ (courtesy of Dr Nathaniel Landau). We thank Reginald Clayton of Tibotec HIV Integrase Discovery group for testing compound with the WT and integrase-resistant HIV-1 viruses. Finally, we thank Yasmeen M. Byrnes for critical reading and editing of the manuscript.

Author contributions

T. A. conducted the research, analysed results and wrote the manuscript. M. P. and D. K. designed and synthesized the PP1-targeting small molecules and contributed to the preparation of the manuscript. A. I., Y. S. K., N. K., K. K-H. and M. J. conducted the research and analysed the results. A. A. K., A. Ü. and D. K. participated in the study design and wrote the manuscript. S. N. takes primary responsibility for the paper. S. N. conducted design and performed some experiments, analysed the results and drafted the manuscript.

Conflict of interest

Patent: Sergei Nekhai, Dmytro Borysovich Kovalskyy 'Inhibitors of protein phosphatase-1 and uses thereof' (U.S. application number: 12/424, 243; publication number: US 2009/0264463 A1).

References

- Alexander SPH, Benson HE, Faccenda E, Pawson AJ, Sharman JL, Spedding M *et al.* (2013). The Concise Guide to PHARMACOLOGY 2013/14: Enzymes. *Br J Pharmacol* 170: 1797–1867.
- Ammosova T, Jerebtsova M, Beullens M, Lesage B, Jackson A, Kashanchi F *et al.* (2005). Nuclear targeting of protein phosphatase-1 by HIV-1 Tat protein. *J Biol Chem* 280: 36364–36371.
- Ammosova T, Berro R, Jerebtsova M, Jackson A, Charles S, Klase Z *et al.* (2006). Phosphorylation of HIV-1 Tat by CDK2 in HIV-1 transcription. *Retrovirology* 3: 78.
- Ammosova T, Obukhov Y, Kotelkin A, Breuer D, Beullens M, Gordeuk VR *et al.* (2011a). Protein phosphatase-1 activates CDK9 by dephosphorylating Ser175. *PLoS ONE* 6: e18985.
- Ammosova T, Yedavalli VR, Niu X, Jerebtsova M, Van Eynde A, Beullens M *et al.* (2011b). Expression of a protein phosphatase 1 inhibitor, cdNIPP1, increases CDK9 threonine 186 phosphorylation and inhibits HIV-1 transcription. *J Biol Chem* 286: 3798–3804.
- Ammosova T, Platonov M, Yedavalli VR, Obukhov Y, Gordeuk VR, Jeang KT *et al.* (2012). Small molecules targeted to a non-catalytic 'RVxF' binding site of protein phosphatase-1 inhibit HIV-1. *PLoS ONE* 7: e39481.
- Barboric M, Lenasi T, Chen H, Johansen EB, Guo S, Peterlin BM (2009). 7SK snRNP/P-TEFb couples transcription elongation with

alternative splicing and is essential for vertebrate development. *Proc Natl Acad Sci U S A* 106: 7798–7803.

Bissantz C, Kuhn B, Stahl M (2010). A medicinal chemist's guide to molecular interactions. *J Med Chem* 53: 5061–5084.

Breuer D, Kotelkin A, Ammosova T, Kumari N, Ivanov A, Ilatovskiy AV *et al.* (2012). CDK2 regulates HIV-1 transcription by phosphorylation of CDK9 on serine 90. *Retrovirology* 9: 94.

Chen R, Yang Z, Zhou Q (2004). Phosphorylated positive transcription elongation factor b (P-TEFb) is tagged for inhibition through association with 7SK snRNA. *J Biol Chem* 279: 4153–4160.

Chen R, Liu M, Li H, Xue Y, Ramey WN, He N *et al.* (2008). PP2B and PP1alpha cooperatively disrupt 7SK snRNP to release P-TEFb for transcription in response to Ca²⁺ signaling. *Genes Dev* 22: 1356–1368.

Debebe Z, Ammosova T, Breuer D, Lovejoy DB, Kalinowski DS, Kumar K *et al.* (2011). Iron chelators of the di-2-pyridylketone thiosemicarbazone and 2-benzoylpyridine thiosemicarbazone series inhibit HIV-1 transcription: identification of novel cellular targets—iron, cyclin-dependent kinase (CDK) 2, and CDK9. *Mol Pharmacol* 79: 185–196.

Deng L, Ammosova T, Pumfery A, Kashanchi F, Nekhai S (2002). HIV-1 Tat interaction with RNA polymerase II C-terminal domain (CTD) and a dynamic association with CDK2 induce CTD phosphorylation and transcription from HIV-1 promoter. *J Biol Chem* 277: 33922–33929.

Gervais A, West D, Leoni LM, Richman DD, Wong-Staal F, Corbeil J (1997). A new reporter cell line to monitor HIV infection and drug susceptibility in vitro. *Proc Natl Acad Sci U S A* 94: 4653–4658.

He N, Jahchan NS, Hong E, Li Q, Bayfield MA, Maraia RJ *et al.* (2008). A La-related protein modulates 7SK snRNP integrity to suppress P-TEFb-dependent transcriptional elongation and tumorigenesis. *Mol Cell* 29: 588–599.

Hendrickx A, Beullens M, Ceulemans H, Den Abt T, Van Eynde A, Nicolaescu E *et al.* (2009). Docking motif-guided mapping of the interactome of protein phosphatase-1. *Chem Biol* 16: 365–371.

Jeronimo C, Forget D, Bouchard A, Li Q, Chua G, Poitras C *et al.* (2007). Systematic analysis of the protein interaction network for the human transcription machinery reveals the identity of the 7SK capping enzyme. *Mol Cell* 27: 262–274.

Kilkenny C, Browne W, Cuthill IC, Emerson M, Altman DG (2010). NC3Rs Reporting Guidelines Working Group. *Br J Pharmacol* 160: 1577–1579.

Kimpton J, Emerman M (1992). Detection of replication-competent and pseudotyped human immunodeficiency virus with a sensitive cell line on the basis of activation of an integrated beta-galactosidase gene. *J Virol* 66: 2232–2239.

Kohoutek J (2009). P-TEFb- the final frontier. *Cell Div* 4: 19.

Krueger BJ, Jeronimo C, Roy BB, Bouchard A, Barrandon C, Byers SA *et al.* (2008). LARP7 is a stable component of the 7SK snRNP while P-TEFb, HEXIM1 and hnRNP A1 are reversibly associated. *Nucleic Acids Res* 36: 2219–2229.

Lafeuillade A, Stevenson M (2011). The search for a cure for persistent HIV reservoirs. *AIDS Rev* 13: 63–66.

Larochelle S, Amat R, Glover-Cutter K, Sanso M, Zhang C, Allen JJ *et al.* (2012). Cyclin-dependent kinase control of the initiation-to-elongation switch of RNA polymerase II. *Nat Struct Mol Biol* 19: 1108–1115.

Li Q, Price JP, Byers SA, Cheng D, Peng J, Price DH (2005). Analysis of the large inactive P-TEFb complex indicates that it contains one

7SK molecule, a dimer of HEXIM1 or HEXIM2, and two P-TEFb molecules containing Cdk9 phosphorylated at threonine 186. *J Biol Chem* 280: 28819–28826.

Markert A, Grimm M, Martinez J, Wiesner J, Meyerhans A, Meyuhas O *et al.* (2008). The La-related protein LARP7 is a component of the 7SK ribonucleoprotein and affects transcription of cellular and viral polymerase II genes. *EMBO Rep* 9: 569–575.

Mbonye UR, Gokulrangan G, Datt M, Dobrowolski C, Cooper M, Chance MR *et al.* (2013). Phosphorylation of CDK9 at Ser175 enhances HIV transcription and is a marker of activated P-TEFb in CD4(+) T lymphocytes. *PLoS Pathog* 9: e1003338.

McGrath J, Drummond G, Kilkenny C, Wainwright C (2010). Guidelines for reporting experiments involving animals: the ARRIVE guidelines. *Br J Pharmacol* 160: 1573–1576.

Nekhai S, Bhat UG, Ammosova T, Radhakrishnan SK, Jerebtsova M, Niu X *et al.* (2007). A novel anticancer agent ARC antagonizes HIV-1 and HCV. *Oncogene* 26: 3899–3903.

Nekhai S, Kumari N, Dhawan S (2013). Role of cellular iron and oxygen in the regulation of HIV-1 infection. *Future Virol* 8: 301–311.

Nekhai S, Petukhov M, Breuer D (2014). Regulation of CDK9 activity by phosphorylation and dephosphorylation. *Biomed Res Int* 2014: 964964.

Nguyen VT, Kiss T, Michels AA, Bensaude O (2001). 7SK small nuclear RNA binds to and inhibits the activity of CDK9/cyclin T complexes. *Nature* 414: 322–325.

Pawson AJ, Sharman JL, Benson HE, Faccenda E, Alexander SP, Buneman OP *et al.*; NC-IUPHAR (2014). The IUPHAR/BPS Guide to PHARMACOLOGY: an expert-driven knowledge base of drug targets and their ligands. *Nucl. Acids Res* 42 (Database Issue): D1098–1106.

Peng J, Zhu Y, Milton JT, Price DH (1998). Identification of multiple cyclin subunits of human P-TEFb. *Genes Dev* 12: 755–762.

Peterson SR, Dvir A, Anderson CW, Dynan WS (1992). DNA binding provides a signal for phosphorylation of the RNA polymerase II heptapeptide repeats. *Genes Dev* 6: 426–438.

Radhakrishnan SK, Gartel AL (2006). A novel transcriptional inhibitor induces apoptosis in tumor cells and exhibits antiangiogenic activity. *Cancer Res* 66: 3264–3270.

Sedore SC, Byers SA, Biglione S, Price JP, Maury WJ, Price DH (2007). Manipulation of P-TEFb control machinery by HIV: recruitment of P-TEFb from the large form by Tat and binding of HEXIM1 to TAR. *Nucleic Acids Res* 35: 4347–4358.

Yang Z, Zhu Q, Luo K, Zhou Q (2001). The 7SK small nuclear RNA inhibits the CDK9/cyclin T1 kinase to control transcription. *Nature* 414: 317–322.

Yang Z, Yik JH, Chen R, He N, Jang MK, Ozato K *et al.* (2005). Recruitment of P-TEFb for stimulation of transcriptional elongation by the bromodomain protein Brd4. *Mol Cell* 19: 535–545.

Supporting information

Additional Supporting Information may be found in the online version of this article at the publisher's web-site:

<http://dx.doi.org/10.1111/bph.12863>

Table S1 Derivatives of 1H4 analysed for HIV-1 inhibition (acridines_rev1.sdf).